euspen's 26th International Conference & Exhibition, Krakow, PL, June 2026
www.euspen.eu

Evaluation of radii in machined components

Adam Szczepański[1], Marek Magdziak[2]

[1]Pratt & Whitney Rzeszów, Poland
[2]Faculty of Mechanical Engineering and Aeronautics, Rzeszów University of Technology, Rzeszów, Poland

adam.szczepanski@prattwhitney.com

Abstract

The paper addresses the requirements specified in the ASME Y14.5-2018 standard concerning the radii of machined parts, with particular emphasis on the controlled radius specification. The controlled radius differs from a regular radius requirement in that it defines not only the nominal size of a radius but also constrains its form and smoothness, excluding flats, reversals, and local irregularities. This type of specification is commonly applied to aerodynamic and rotating components, where geometric continuity and smooth surface transitions are critical. This paper investigates the influence of profile deviations in a radius curve on the measured radius value obtained using CMM scanning. A reference object containing several radii with intentionally simulated defects in the form of flattened areas was scanned under various measurement strategies. The scanning velocities were varied to evaluate their influence on the radii evaluated in accordance with the selected requirement specified in ASME Y14.5-2018.

Keywords: controlled radius, CMM, scanning

1. Introduction

The aerospace industry faces a growing challenge in maintaining the highest levels of operational safety while continuously pursuing weight reduction, increased energy efficiency, and extended engine lifetime. One of the key factors influencing the reliability of rotating assemblies is the dimensional and geometric accuracy of their mechanical components, particularly in surface regions that are critical to fluid flow, stress distribution, and fatigue resistance. Even minor deviations in curvature transitions can result in stress concentrations, which may subsequently initiate cracks and lead to component failure during engine operation [1].

Within this context, the proper definition and control of transitional radii become essential. According to ASME Y14.5–2018 [2], the Controlled Radius (CR) measurement characteristic may be used for such a task. The CR is defined as a smoothly blended transition between two surfaces, free from reversals of curvature or local discontinuities, while maintaining the radius value within specified tolerance limits throughout the entire feature.

The subsequent sections of the paper present:

- a comparison of various methods used to define radius requirements,
- the experiments carried out using a coordinate measuring machine (CMM), with measurements performed on a specially designed object containing different curvatures and intentional defects,
- final conclusions regarding the conducted investigations.

2. Radius requirements discussion

In geometric dimensioning and tolerancing (GD&T), as specified in [2], there are three primary methods used to define a radius. The first and most traditional method, applied for many years, is the standard radius, which allows a profile to assume essentially any shape as long as it lies within a crescent-shaped tolerance zone (in cases where the center of the radius is not specified). The interpretation of this type of requirement is shown in Figure 1. However, this approach does not guarantee the continuity or smoothness of a profile and is therefore inadequate for sufficiently constraining local variations in curvature.

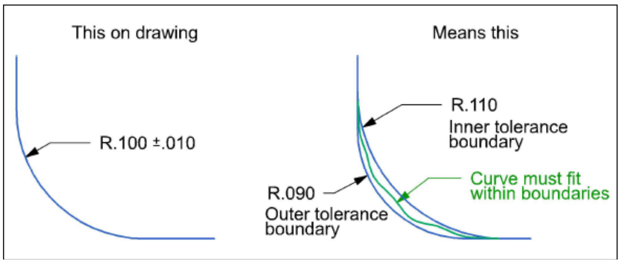

Figure 1. Definition of the standard radius [2]

Another possibility is the application of profile of a line tolerance to control the radius. The tolerance zone is created by offsetting the basic radius-shaped curve by a value equal to half of the specified profile tolerance on both sides. This method is often preferred from a metrological point of view, as it guarantees repeatable and consistent inspection results, unlike the standard method, where the results may vary significantly due to changes in the curvature. However, this approach is less suitable when the objective is to limit distortions in the shape of a curve. The interpretation of this characteristic is shown in Figure 2.

The CR was introduced to limit distortions of the radius of a curve and to ensure uniform stress distribution along the transition. The standard [2] defines the CR requirements but does not provide any detailed guidelines for inspection methods. The key question is to what extent an imperfection constitutes a violation of the CR specification. Therefore, it is recommended that such limits should be defined in company standards or equivalent internal documents. The interpretation of the CR characteristic is illustrated in Figure 3. A method for assessing this characteristic was proposed in [3].

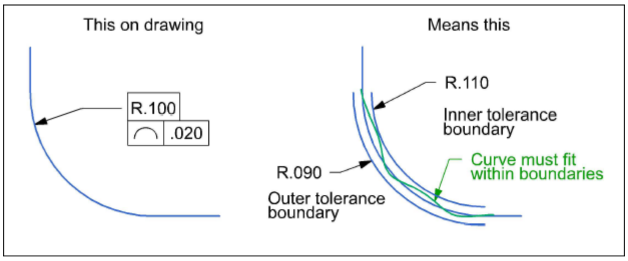

Figure 2. Profile of a line controlling a radius [2]

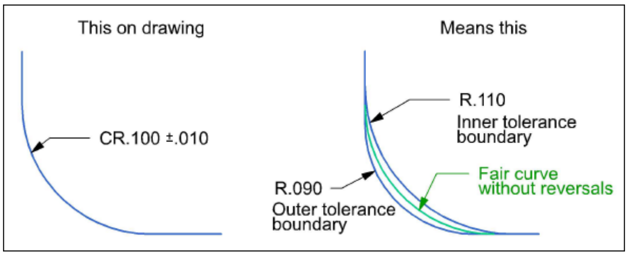

Figure 3. Interpretation of the controlled radius [2]

The evaluation path may be composed of the stages presented in Figure 4. It should be noted that the same method can be used to determine the actual radius value for both R and CR, however, CR requires radius defects evaluation, which is not required for an ordinary radius.

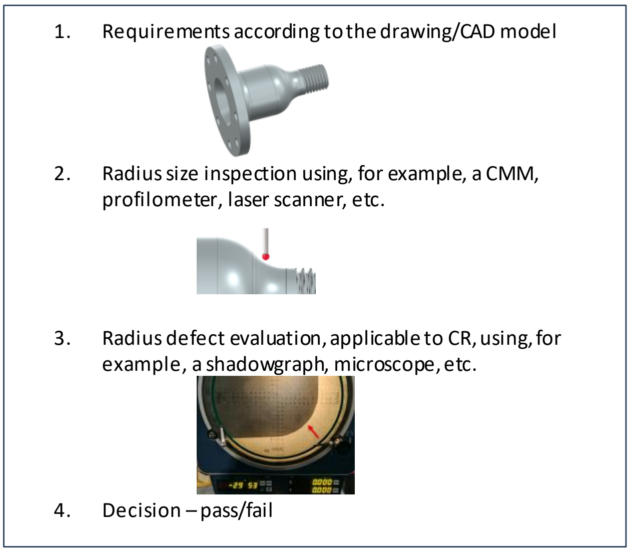

Figure 4. Radius evaluation steps for the CR characteristic

In another study, the authors investigated the standardization of CR evaluation by involving three professional quality inspectors to assess the consistency of their judgments and to develop an acceptance matrix. A shadowgraph equipped with a 20× magnification lens was used for the examination, enabling the inspectors to identify very small defects. The detection threshold was established using the same artifact presented in this paper. In addition, the use of a coordinate measuring machine for the evaluation of defects of the inspected radius was also investigated.

3. Experimental investigation

The purpose of the experiment described herein is to determine how defects located on a radius curve affect the repeatability of inspection results at various scanning speeds when using a coordinate measuring machine. The inspection was carried out on an artifact specifically designed for this purpose.

3.1. Examined object

The reference object containing curves with radii ranging from R=2 mm to R=20 mm was designed, see Figure 5. The radii were intentionally distorted to introduce controlled defects in the form of flattened regions, with depths ranging from 0.005 mm to 0.08 mm. The artifact was manufactured as a sheet metal component using wire electrical discharge machining (wire EDM) to ensure high dimensional accuracy.

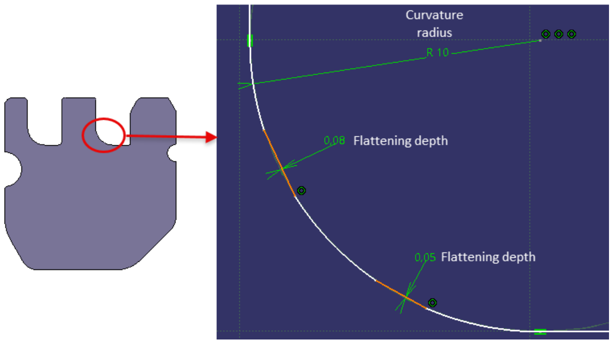

Figure 5. Reference object and an example of a simulated radius defect

Table 1 summarizes the defects. It should be noted that the radii were located at corners with different angles as presented in Figure 6, and in many cases more than one defect was present on a single curve.

Table 1. Summary of radii and defect sizes

Radius index	Radius size [mm]	Defect size [mm]	R at corner angle [deg]
B4	2	0.01	120
B10	2	0.015; 0.02	90
B11	2	0.05	90
B17	2	0	115
B5	5	0.005; 0.01; 0.015	120
B6	5	0	150
B14	5	0.02; 0.025; 0.03	90
B1	5	0	not in corner, groove radius
B8	10	0.005; 0.01; 0.015; 0.02; 0.03	90
B12	10	0.05; 0.08	90
B16	10	0	not in corner, groove radius
B19	10	0.05	120
B21	10	0.08	135

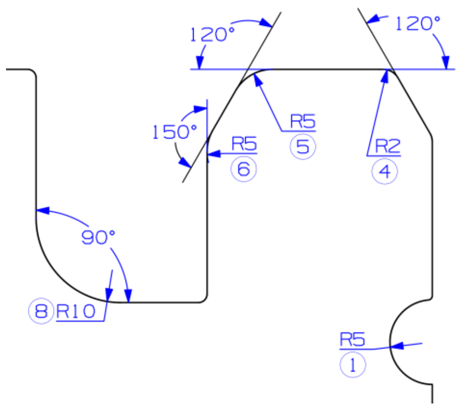

Figure 6. Fragment of the artifact with marked comer angles

3.2. CMM inspection

The contour of the reference object was scanned using a CMM equipped with a VAST Gold active scanning head, controlled by Calypso software. The scanning path was based on the CAD model of the artifact, with a point resolution of 0.02 mm. A ruby stylus with a diameter of 0.5 mm was used, and no software filtering was applied. In order to calculate the values of actual radii the Gaussian fitting algorithm was selected. Three scanning speeds: 10 mm/s, 5 mm/s, and 1 mm/s were applied, and ten repeated measurements were carried out for each speed in order to evaluate repeatability. The resulting scans were then used to measure two types of radius characteristics: R and CR as well as a line profile. R and CR were identical in terms of radius size evaluation. Figure 7 shows the artifact during the CMM scanning process.

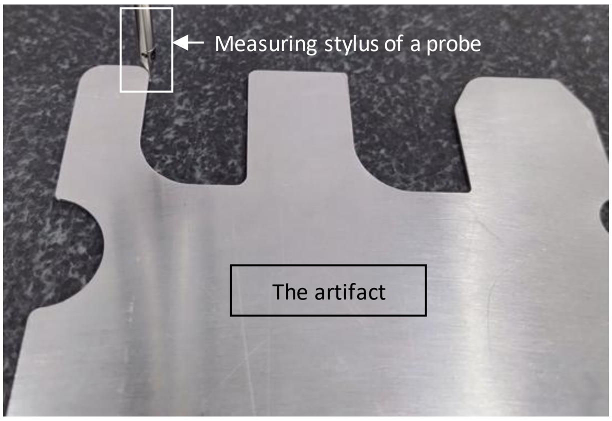

Figure 7. CMM Inspection

4. Results of investigations

Figure 8 presents the results of the radius value inspection, illustrating the influence of the applied scanning speed and simulated defects on the variation of the measured radius values. Since the evaluation method is identical for both R and CR, the obtained results are also identical. However, within a standard quality inspection process, CR requires additional assessment of profile defects (like presented in Figure 4).

The experiment reveals that the scanning speed within the assumed range has a limited influence on the observed variation. Although it could be expected that the stability at 1 mm/s would be better than at 10 mm/s, the measured values do not confirm such an assumption in all cases. There are examples in which the scanning speed has only a negligible effect on the variation, as observed for radii B10, B17, B8, and B16.

In some cases, the differences in variation between individual scanning speeds were clearly noticeable, however, there is no consistent trend supporting the claim that the variation increases with increasing speed. There are even examples in which a lower scanning speed resulted in greater variation, as can be seen for B11 and B5.

The variation observed for B1 at 10 mm/s and for B12 at 5 mm/s appears to be random, as it is significantly different from the values obtained at the two remaining scanning speeds. Nevertheless, B12 contains two significant defects (0.05 mm and 0.08 mm), which makes this radius more susceptible to increased variation. This leads to the conclusion that the highest variation is generally associated with larger defect sizes. A similar relationship can also be observed for other radii, such as B11 (defect of 0.05 mm), B19 (defect of 0.05 mm), and B21 (defect of 0.08 mm).

This effect is additionally strengthened by the fact that these curves are located at corners with obtuse angles. This is a well-known phenomenon affecting coordinate-based inspection methods, including CMMs, profilometers, laser scanners, and similar systems. In general, the wider the included angle, the poorer the repeatability of the inspection results.

The results of the line profile evaluation are presented in Figure 9. The same data points that were used for the actual radius calculation were also applied for the profile computation. The profile of each curve was best fitted to the nominal curve using Gaussian method.

It is immediately visible that, compared with the actual radius value evaluation, the line profile results are more stable across the entire range of radii and scanning speeds. There is one case for B10 in which the variation at 1 mm/s significantly differs from the values obtained for the other two scanning speeds, therefore, it can be regarded as an exceptional result.

The most interesting portion of the data is related to the radii with a nominal size of 10 mm. Although B8 contains numerous defects and B12 includes the largest individual defects, the variation remains at a very low level for both radii. These two features are located at corners with a right angle.

A reduction in the repeatability of the profile results can be observed for B16, B19, and B21. The radius indexed as B16 is not located at a corner but represents a groove radius. It contains the highest number of inspection points, which is generally considered beneficial in coordinate metrology. On the other hand, a larger number of points also increases the likelihood that random deviations may influence the result. Unlike the calculation of the actual radius using the Gaussian fitting method, where the result is effectively averaged, profile evaluation is more sensitive because each individual point contributes directly to the final value.

For B19 and B21, which are located at corners with obtuse angles, the variation occurs at a level comparable to that observed for B16, and it also correlates with the variation of the R value inspection results. For B19, in both evaluation methods, the highest variation is visible at 5 mm/s, whereas for B21 the highest variation occurs at 10 mm/s. This leads to the conclusion that, for both methods, the quality of the scanned data has a greater influence on the results than the applied evaluation method.

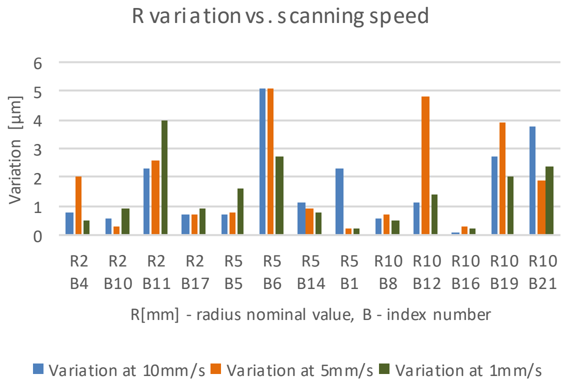

Figure 8. Radius actual value variation for different scanning speeds and radii sizes

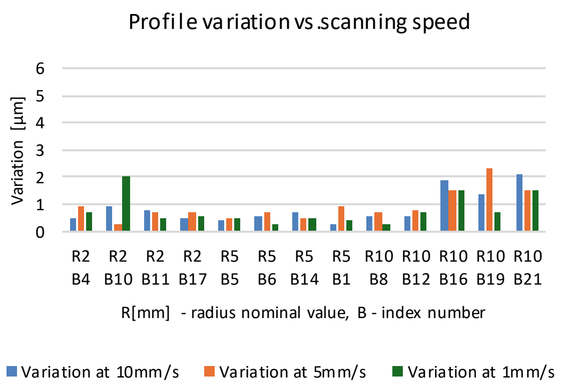

Figure 9. Radius profile variation for different scanning speeds and radii sizes

5. Conclusions

The conducted experiments revealed that the measurement results depend on the applied scanning speed only to a limited extent. Although scanning speed may have an influence on the measured values, the measuring system and software used in the study appear to minimize this effect, thereby limiting the dispersion of the obtained data. When scanning with the active VAST Gold probe, the system automatically adjusts the actual scanning speed to the local curvature of the measured feature, even if a higher nominal scanning speed has been defined in the software. As a result, the probe slows down in regions with smaller radii or more complex geometry, which improves contact stability and reduces the influence of the programmed scanning speed on the final measurement results. The most significant variation in radius values (for the standard radius characteristic) was observed for curves containing the largest simulated manufacturing defects.

The comparison between the two evaluation methods (actual radius value computation and line profile assessment), shows that the second one provides less variable results. The repeatability of the profile results, typically below one micrometer and only in a few cases between one and two micrometers, supports this conclusion.

Further investigations will focus on the analysis of defect detection levels, including other typical defects such as mismatch, double R, cusp, and similar irregularities. Additional research will address the development of advanced algorithms for automated CR evaluation within coordinate inspection systems. The authors plan to continue this work in collaboration with an aviation industry company producing safety-critical rotating components.

References

[1] National Transportation Safety Board (NTSB), 2023, Aviation Investigation Final Report: Accident Number WPR22LA019,

[2] The American Society of Mechanical Engineers (ASME), 2018, ASME Y14.5-2018: Dimensioning and Tolerancing Engineering Product Definition and Related Document Practices

[3] Magdziak M. 2024, Application of Coordinate Measuring Machines for Analysis of a Controlled Radius Based on Linear Regression, Adv. Sci. Technol. Res. J. **18(2)** 11-25